The Tungsten−Tungsten Triple Bond. 20.[1] Synthesis and Characterization of Cyclooctatetraenyltetrakis(dimethylamido)ditungsten

Roger H. Cayton, Stephanie T. Chacon, Malcolm H. Chisholm,* and Kirsten Folting

Department of Chemistry and Molecular Structure Center, Indiana University, Bloomington, Indiana 47405

Kandasamy G. Moodley

Department of Chemistry, University of Durban-Westerville, P/Bag X54001, Durban 4000, South Africa

Received November 7, 1995[⊗]

The reaction between Li_2COT, where COT = c-C_8H_8, and $W_2Cl_2(NMe_2)_4$ yields $W_2(\mu\text{-}\eta^5,\eta^5\text{-}C_8H_8)(NMe_2)_4$, which has been characterized in the solid-state and in solution. The solid-state structure is described as being derived from a $C_8H_8^{4-}$ anion coordinated to a W_2^{8+} template, and this is supported by a Fenske−Hall molecular orbital calculation. In solution the molecule is fluxional as the tub-shaped C_8H_8 ring moves about the W_2 center and interconverts with another isomer.

Introduction

The coordination chemistry associated with the central W_2^{6+} center is extremely rich, and those compounds containing W≡W bonds provide versatile templates for the coordination of unsaturated organic molecules.[2] In a previous report we described the coordination of allyl and pentadienyl ligands in compounds of formula $W_2R_2(NMe_2)_4$.[3] The allyl ligands were capable of coordinating in a variety of modes, specifically as 1,2-$W_2(\eta^1\text{-}R)_2(NMe_2)_4$, 1,2-$W_2(\eta^3\text{-}R)_2(NMe_2)_4$, and $W_2(\mu\text{-}R)_2(NMe_2)_4$. In the latter case the bridging allyl ligand straddled the W−W bond in a similar manner to that seen in $M_2(\mu\text{-}C_3H_5)_2(\eta^3\text{-}C_3H_5)_2$ complexes where M = Cr[4] and Mo[5] and C_3H_5 = allyl. As is shown in A, there are two cis

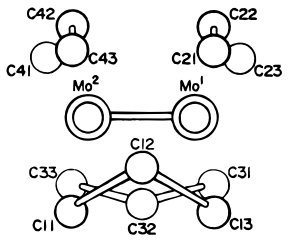

A

bridging allyl groups. In this geometry there is a maximum of mixing between M−M and M−allyl bonding. Indeed the allyl π^* MO has the appropriate symmetry to receive electron density from the filled M−M π-bonding MO's. This form of metal-to-ligand π-back-bonding is evidently important since the M−M distance is that of a M−M double bond and the C−C distances are approaching those normally seen for $C_{sp^2}-C_{sp^2}$ single bonds.

The cyclooctatetraene ligand, C_8H_8 = COT, is nonaromatic, but the dianion, COT^{2-}, is planar as is seen in $U(COT)_2$.[6] It is also known to adopt interesting modes of bonding in dinuclear complexes such as $M_2(COT)_3$, where M = Cr,[7] and W,[8,9] which have M−M distances of 2.214(11), 2.302(2), and 2.375(1) Å, respectively. All share a common structure wherein two of the COT ligands are terminally bonded to each metal atom in an η^4-C_8H_8 mode while the third COT bridges the two metal atoms in a μ-η^5-C_8H_8 mode as shown in B.

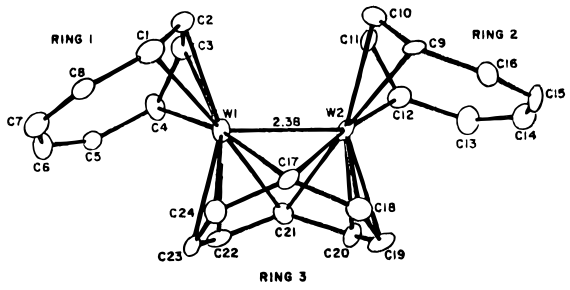

B

The bridging COT ligand bears some analogy to the bis(μ-allyl)−M_2 moiety in $W_2(\mu\text{-}C_3H_5)_2(NMe_2)_4$ shown in C, and so we felt it was important to prepare a compound of formula $W_2(COT)(NMe_2)_4$ to interrogate

[⊗] Abstract published in *Advance ACS Abstracts,* January 1, 1996.

(1) Part 19: Chisholm, M. H.; Kramer, K. S.; Martin, J. D.; Huffman, J. C.; Labkovsky, E. B.; Streib, W. E. *Inorg. Chem.* **1992**, *31*, 4469.

(2) (a) Chisholm, M. H. *Acc. Chem. Res.* **1990**, *23*, 419. (b) Chisholm, M. H. *J. Organomet. Chem.* **1990**, *400*, 235.

(3) (a) Chisholm, M. H.; Hampden-Smith, M. J.; Huffman, J. C.; Moodley, K. G. *J. Am. Chem. Soc.* **1988**, *110*, 4070. (b) Cayton, R. H.; Chisholm, M. H.; Hampden-Smith, M. J.; Huffman, J. C.; Moodley, K. G. *Polyhedron* **1992**, *11*, 3197.

(4) (a) Aoki, T.; Furusaki, A.; Tomiie, Y.; Ono, K.; Tanaka, K. *Bull. Soc. Chim. Jpn.* **1969**, *42*, 545. (b) Albrecht, G.; Stock, D. *Z. Chem.* **1967**, *7*, 32.

(5) Cotton, F. A.; Troup, J. M.; Webb, T. R.; Williamson, D. H.; Wilkinson, G. *J. Am. Chem. Soc.* **1974**, *96*, 3824.

(6) Raymond, K. N.; Eigenbrot, C. W., Jr. *Acc. Chem. Res.* **1980**, *13*, 276.

(7) Bramer, D. J.; Kruger, C. *Inorg. Chem.* **1976**, *15*, 2511.

(8) Cotton, F. A.; Koch, S. A.; Schultz, A. J.; Williams, J. M. *Inorg. Chem.* **1978**, *17*, 2093.

(9) Cotton, F. A.; Koch, S. A. *J. Am. Chem. Soc.* **1977**, *99*, 7371.

0276-7333/96/2315-0992$12.00/0

the nature of the COT to W_2 bonding. We describe herein our findings.

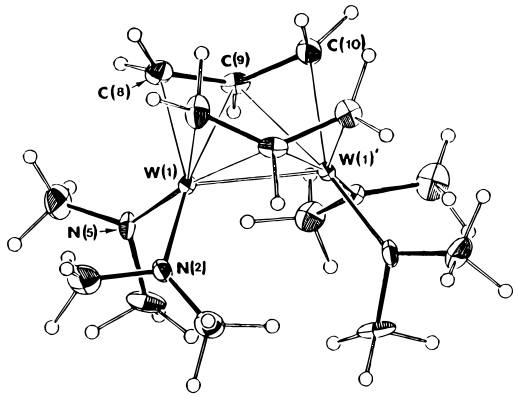

C

Results and Discussion

Syntheses. From the reaction between 1,2-$W_2Cl_2(NMe_2)_4$ and $Li_2(COT)$ in tetrahydrofuran (THF) at 0 °C the green compound $W_2(COT)(NMe_2)_4$ was formed and obtained as green crystals from toluene in ca. 60% yield based on tungsten, eq 1.

$$1,2\text{-}W_2Cl_2(NMe_2)_4 + Li_2C_8H_8 \xrightarrow[THF]{0\ °C} W_2(COT)(NMe_2)_4 + 2LiCl \quad (1)$$

If an excess of Li_2COT is used, then the previously reported compound $W_2(COT)_3$[8,9] is formed. Rather interestingly, attempts to prepare the related $Mo_2(COT)(NMe_2)_4$ by the same procedure but with 1,2-$Mo_2Cl_2(NMe_2)_4$ were unsuccessful. The only COT-containing compound to be isolated was $Mo_2(COT)_3$. The bonding in $M_2(COT)_3$, where M = Cr, Mo, and W, has been previously described[8,9] in terms of a M−^{4}M bond, and thus the relative ease of reduction of Mo(III) relative to W(III) may account for the preferential formation of $Mo_2(COT)_3$.

Solid-State and Molecular Structure of $W_2(COT)(NMe_2)_4$. In the space group $P2_1/a$ there is one unique molecule in the asymmetric unit. Atomic coordinates are listed in Table 1, and pertinent bond distances and bond angles are given in Tables 2 and 3. An ORTEP drawing of the molecule giving the atom number scheme is given in Figure 1. The molecule has no crystallographically imposed symmetry though there is an approximate C_2 axis as is perhaps best shown by the view of the molecule presented in Figure 2. From an inspection of Figures 2 and 3 it is clear (1) that there are two types of NMe_2 ligands distinguished primarily by the dihedral angle of their NC_2 planes with respect to the W−W axis and (2) that the μ-C_8H_8 ligand can be viewed as being derived from the bis(allyl) complex $W_2(\mu\text{-}C_3H_5)_2(NMe_2)_4$ wherein C(5)−H or C(9)−H replace C−H bonds to link the allyl ligands and generate μ-C_8H_8. Two stereodrawings of the best superposition of the $W_2(\mu\text{-allyl})_2(NMe_2)_4$ and $W_2(\mu\text{-COT})(NMe_2)_4$ molecules are given in Figure 3. The closeness of fit is really quite remarkable.

Remarks on Bonding. Planar $C_8H_8^{2-}$ is aromatic with an occupied e_π molecular orbital of a nonbonding character as the HOMO. A splitting of the e orbitals occurs upon distortion from planarity, and the π MOs of the COT bent in the shape of the C_8 skeleton that bridges the two metal atoms in $W_2(COT)(NMe_2)_4$ are shown in Figure 4.

Table 1. Fractonal Coordinates and Isotropic Thermal Parameters (Å^2) for $W_2(COT)(NMe_2)_4$

atom	10^4x	10^4y	10^4z	$10B_{iso}$
W(1)	5362.9(5)	1594.1(1)	5931.5(4)	9
W(2)	4354.0(5)	843.3(1)	5730.4(4)	8
C(3)	7243(12)	1066(3)	8164(12)	15
C(4)	8299(13)	1419(3)	7889(12)	15
C(5)	8417(14)	1540(3)	6364(14)	16
C(6)	7128(14)	1451(4)	4584(14)	20
C(7)	5778(13)	1112(3)	3876(12)	13
C(8)	6045(13)	649(3)	4321(12)	13
C(9)	6934(12)	448(3)	6006(13)	13
C(10)	7195(13)	617(3)	7634(13)	15
N(11)	3454(10)	1930(3)	4023(10)	13
C(12)	2105(15)	1774(4)	2306(13)	20
C(13)	3393(14)	2406(3)	4004(14)	18
N(14)	4945(11)	1960(3)	7705(10)	15
C(15)	3088(16)	2108(4)	7408(15)	22
C(16)	6233(16)	2052(4)	9521(14)	24
N(17)	3218(11)	747(3)	7296(10)	14
C(18)	2123(15)	353(3)	7219(15)	18
C(19)	3540(17)	986(4)	8879(14)	20
N(20)	1899(11)	700(3)	3610(10)	13
C(21)	1592(14)	560(3)	1881(13)	16
C(22)	87(13)	828(4)	3504(13)	16

Table 2. Selected Bond Distances (Å) for $W_2(COT)(NMe_2)_4$

W(1)−W(2)	2.4297(5)	W(2)−N(17)	1.949(8)
W(1)−N(11)	1.960(7)	W(2)−N(20)	2.041(8)
W(1)−N(14)	2.031(8)	W(2)−C(3)	2.420(9)
W(1)−C(3)	2.445(9)	W(2)−C(7)	2.473(9)
W(1)−C(4)	2.262(9)	W(2)−C(8)	2.260(9)
W(1)−C(5)	2.316(10)	W(2)−C(9)	2.322(9)
W(1)−C(6)	2.232(10)	W(2)−C(10)	2.239(9)
W(1)−C(7)	2.431(9)		

The frontier MOs of the $W_2(NMe_2)_4^{2+}$ fragment are shown in Figure 5. These were calculated with the geometry of a $W_2(NH_2)_4$ fragment taken from the structure of $W_2(COT)(NMe_2)_4$ employing the method of Fenske and Hall. Also shown in Figure 5 is the interaction diagram wherein $W_2(COT)(NH_2)_4$ is formed from the coupling of the two fragments. The μ-$C_8H_8^{2-}$ orbitals, π_1, π_2, π_3, π_5, π_7, and π_8, can be considered to be analogous to the six π-allyl orbitals shown in **D**. Only

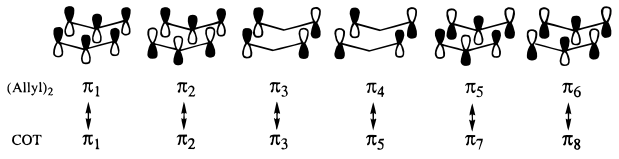

D

the μ-$C_8H_8^{2-}$ orbitals π_4 and π_6 are different. The μ-$C_8H_8^{2-}$ π_6 finds no good match with the W_2 fragment and causes no real bonding problems. However, μ-$C_8H_8^{2-}$ π_4 fights with the μ-$C_8H_8^{2-}$ π_8 for the W−W π-bonding orbital $2a_1$. In the bis(allyl) complex the π_6(allyl) combination is empty and thus back accepts electron density from the W−W π bond. This is further aided by the twisting of the NC_2 blades. However for the μ-$C_8H_8^{2-}$ ligand the filled π_4 MO is close in energy with the M−M π orbital (2a′) and this sets up a filled−filled orbital interaction that pushes the W-based orbital 5a′, the HOMO, rather high in energy. Thus the extra 2 π MOs that come with the μ-$C_8H_8^{2-}$ ligand and are at the C_{sp^2} atoms that point up above each W atom are not

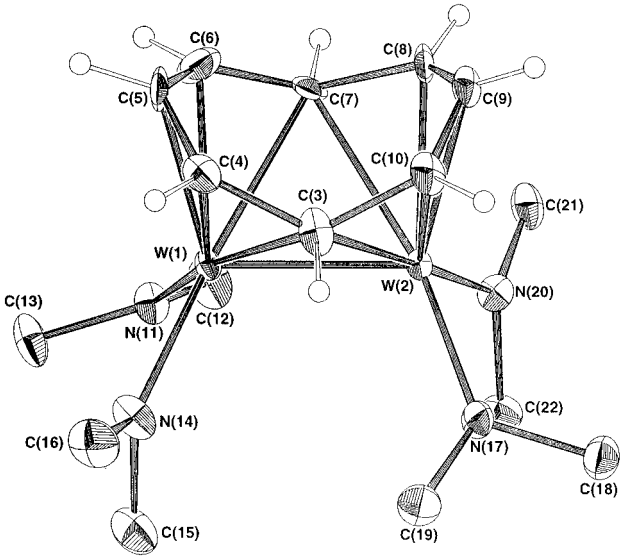

Figure 1. ORTEP drawing of the $W_2(COT)(NMe_2)_4$ molecule giving the atom number scheme.

Table 3. Selected Bond Angles (deg) for $W_2(COT)(NMe_2)_4$

W(2)−W(1)−N(11)	109.33(23)	C(3)−W(2)−C(8)	87.6(3)
W(2)−W(1)−N(14)	114.77(25)	C(3)−W(2)−C(9)	66.0(3)
W(2)−W(1)−C(3)	59.54(22)	C(3)−W(2)−C(10)	36.0(3)
W(2)−W(1)−C(4)	91.68(26)	C(7)−W(2)−C(8)	35.8(3)
W(2)−W(1)−C(5)	103.83(22)	C(7)−W(2)−C(9)	66.0(3)
W(2)−W(1)−C(6)	92.6(3)	C(7)−W(2)−C(10)	87.5(3)
W(2)−W(1)−C(7)	61.17(22)	C(8)−W(2)−C(9)	36.3(3)
N(11)−W(1)−N(14)	89.9(3)	C(8)−W(2)−C(10)	69.2(3)
N(11)−W(1)−C(3)	168.4(3)	C(9)−W(2)−C(10)	35.9(3)
N(11)−W(1)−C(4)	155.4(3)	W(1)−N(11)−C(12)	127.9(7)
N(11)−W(1)−C(5)	123.3(3)	W(1)−N(11)−C(13)	123.1(6)
N(11)−W(1)−C(6)	96.7(4)	W(1)−N(14)−C(15)	122.5(6)
N(11)−W(1)−C(7)	91.7(3)	W(1)−N(14)−C(16)	128.8(7)
N(14)−W(1)−C(3)	92.1(3)	W(2)−N(17)−C(18)	123.0(6)
N(14)−W(1)−C(4)	92.7(3)	W(2)−N(17)−C(19)	128.0(7)
N(14)−W(1)−C(5)	115.9(3)	W(2)−N(20)−C(21)	128.7(6)
N(14)−W(1)−C(6)	148.0(4)	W(2)−N(20−C(22)	122.2(6)
N(14)−W(1)−C(7)	175.9(3)	W(1)−C(3)−W(2)	59.92(20)
C(3)−W(1)−C(4)	35.8(3)	W(1)−C(3)−C(4)	65.2(5)
C(3)−W(1)−C(5)	65.7(3)	W(1)−C(3)−C(10)	118.0(6)
C(3)−W(1)−C(6)	87.6(4)	W(2)−C(3)−C(4)	118.4(6)
C(3)−W(1)−C(7)	85.5(3)	W(2)−C(3)−C(10)	65.2(5)
C(4)−W(1)−C(5)	35.5(4)	C(4)−C(3)−C(10)	126.5(9)
C(4)−W(1)−C(6)	69.0(4)	W(1)−C(4)−C(3)	78.9(5)
C(4)−W(1)−C(7)	87.4(3)	W(1)−C(4)−C(5)	74.3(6)
C(5)−W(1)−C(6)	36.6(4)	C(3)−C(4)−C(5)	129.4(9)
C(5)−W(1)−C(7)	66.1(3)	W(1)−C(5)−C(4)	70.1(5)
C(6)−W(1)−C(7)	35.4(4)	W(1)−C(5)−C(6)	68.5(5)
W(1)−W(2)−N(17)	109.88(23)	C(4)−C(5)−C(6)	128.3(9)
W(1)−W(2)−N(20)	115.32(23)	W(1)−C(6)−C(5)	74.9(6)
W(1)−W(2)−C(3)	60.54(22)	W(1)−C(6)−W(7)	79.9(5)
W(1)−W(2)−C(7)	59.45(21)	C(5)−C(6)−C(7)	129.8(9)
W(1)−W(2)−C(8)	91.65(22)	W(1)−C(7)−W(2)	59.39(20)
W(1)−W(2)−C(9)	103.74(23)	W(1)−C(7)−C(6)	64.7(5)
W(1)−W(2)−C(10)	92.57(25)	W(1)−C(7)−C(8)	117.2(6)
N(17)−W(2)−N(20)	90.7(3)	W(2)−C(7)−C(6)	117.0(6)
N(17)−W(2)−C(3)	91.0(3)	W(2)−C(7)−C(8)	64.2(5)
N(17)−W(2)−C(7)	169.1(3)	C(6)−C(7)−C(8)	127.2(9)
N(17)−W(2)−C(8)	154.4(3)	W(2)−C(8)−C(7)	80.1(5)
N(17)−W(2)−C(9)	121.4(3)	W(2)−C(8)−C(9)	74.2(5)
N(17)−W(2)−C(10)	95.3(3)	C(7)−C(8)−C(9)	129.1(8)
N(20)−W(2)−C(3)	175.9(3)	W(2)−C(9)−C(8)	69.5(5)
N(20)−W(2)−C(7)	92.5(3)	W(2)−C(9)−C(10)	68.8(5)
N(20)−W(2)−C(8)	92.4(3)	C(8)−C(9)−C(10)	128.2(9)
N(20)−W(2)−C(9)	116.1(3)	W(2)−C(10)−C(3)	78.8(5)
N(20)−W(2)−C(10)	147.5(3)	W(2)−C(10)−C(9)	75.2(5)
C(3)−W(2)−C(7)	85.1(3)	C(3)−C(10)−C(9)	129.2(9)

stabilizing. Indeed this probably contributes to the fluxionality (see later). A mere 45° rotation tranforms

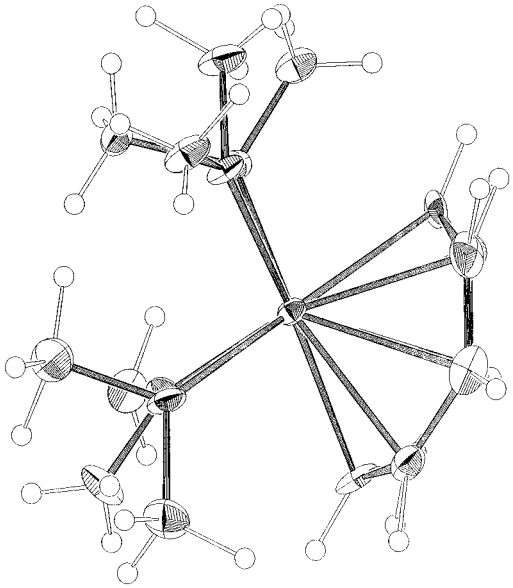

Figure 2. View of the $W_2(COT)(NMe_2)_4$ molecule looking down the M−M bond and showing the near-C_2 symmetry of the molecule.

π_4 into π_5, and the bonding in these two orbitals would remain the same.

NMR Studies. ^1H and ^{13}C NMR data for $W_2(COT)(NMe_2)_4$ are given in the Experimental Section. At 500 MHz and room temperature and in toluene-d_8 the only significant feature in the ^1H NMR spectrum is a broad singlet at δ 3.12 assignable to amido methyl protons. A closer inspection reveals a very broad resonance centered at around δ 5.0 which is almost in the baseline. Upon increasing the temperature, these signals sharpen and give two singlets consistent with the presence of a fluxional molecule.

Upon lowering the temperature, it is evident that there are two isomers present in solution. Both are in rapid equilibrium at room temperature on the NMR time scale. At −40 °C the isomers are in the concentration ratio of 4:3. The major isomer shows three COT resonances at δ 5.80, 5.29, and 3.77 with a relative intensity 1:2:1, respectively. There is a single NMe_2 resonance associated with this isomer, seen at lower temperatures, and so rotations about the M−N bond must be rapid [as was seen for $W_2(\mu\text{-allyl})_2(NMe_2)_4$]. This being the case the molecule has approximate mirror symmetry (pseudo-C_{2v}) as shown in **Ia**,**b**. The COT protons are H_a(4H), H_b(2H), and H_c(2H). H(b) and H(c) appear as triplets, and H(a) appear as a doublet of doublets.

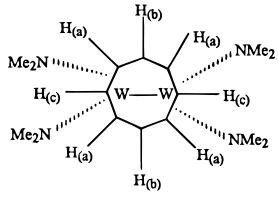

Ia

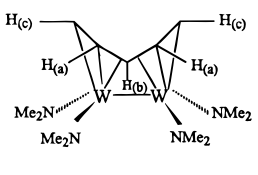

Ib

At low temperatures the other isomer shows two NMe_2 groups of equal integral intensity and four COT signals (2H:2H:2H:2H). NOE experiments indicated the proximity of H(f) and H(e), H(f) and H(g), but no NOE was seen between the COT protons and the NMe_2

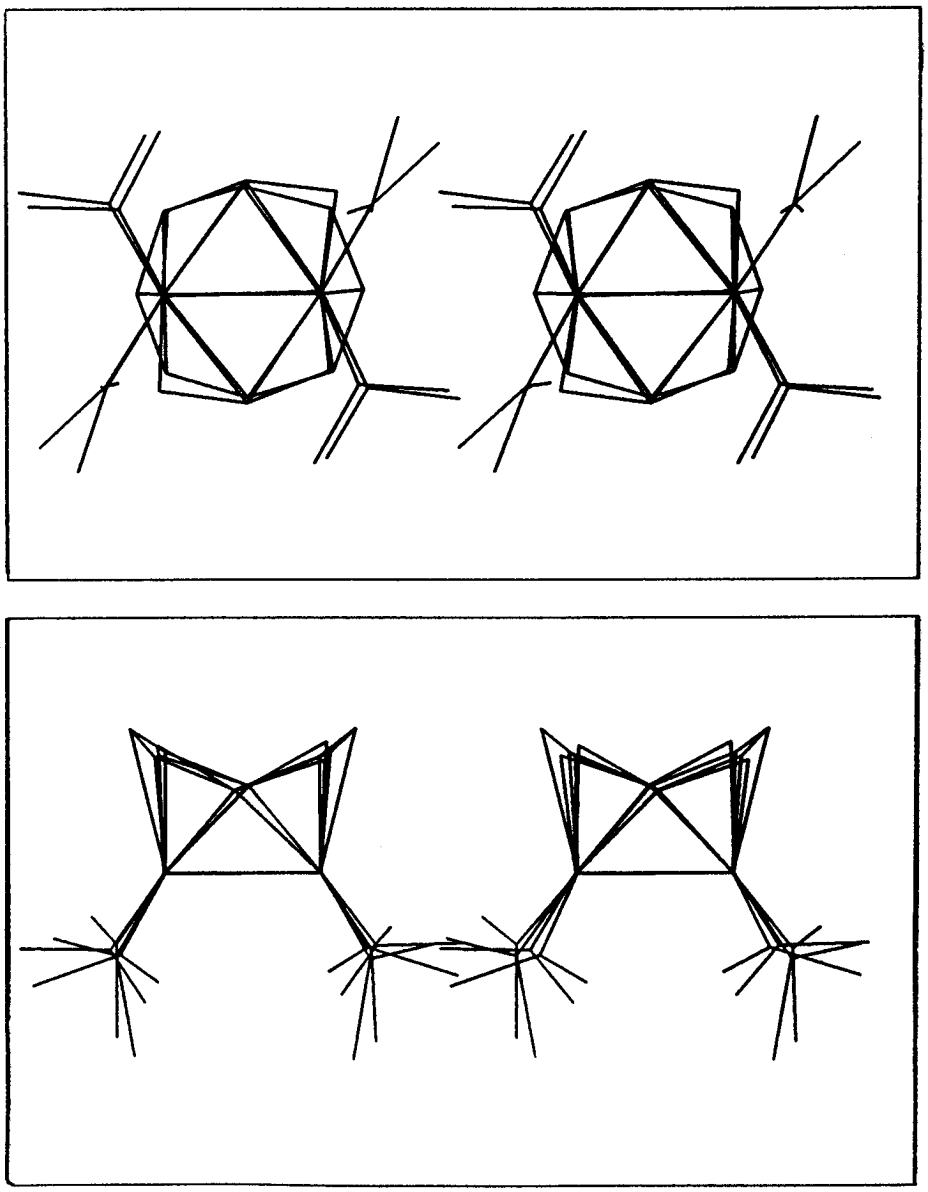

Figure 3. Two stereoviews of the best fit of the $W_2(\mu\text{-allyl})_2(NMe_2)_4$ and $W_2(COT)(NMe_2)_4$ molecule.

protons. Again it is possible to propose a structure having mirror symmetry but now with the COT ligand slipped from the W_2 center so as to have a free olefinic functionality that is not directly bonded to tungsten. ^1H resonances at δ 1.0, 2.2, 3.2, and 7.3 certainly imply a range of very different chemical environments. Two plausible structures are shown in **IIa**,**b**.

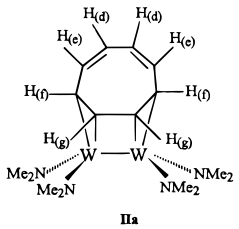

IIa

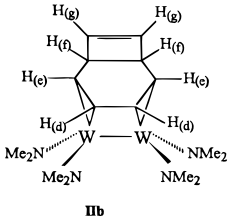

IIb

It should be noted that because of the existence of two isomers in solution we were careful to verify that the spectra were reproducible. Furthermore, crystals from an analytically pure sample were selected and examined by X-ray diffraction to determine that they had the same cell parameters as the one employed in the single-crystal diffraction study. These were then used in an NMR study.

Concluding Remarks. The structure of the $W_2(COT)(NMe_2)_4$ molecule bears a striking similarity to that of the $W_2(\mu\text{-allyl})_2(NMe_2)_4$ molecule. The W−W distance of 2.43 Å is approaching that normally associated with a $(W{=}W)^{8+}$ moiety, and as such, the COT ligand may be viewed as $C_8H_8^{4-}$ which one would expect to be nonplanar. The existence of two isomers in solution and their facile interconversion once again emphasizes the flexibility of the W_2^{n+} center as a template for the binding of unsaturated molecules. It is regrettable that we cannot uniquely define the bonding in the other isomer, but the pictorial descriptions **IIa**,**b** emphasize that metal−ligand bonding may be maximized by local W−C interactions at the expense of the more localized μ-C_8H_8 bonding seen in the crystal structure and described in terms of the orbital integration diagram shown in Figure 4.

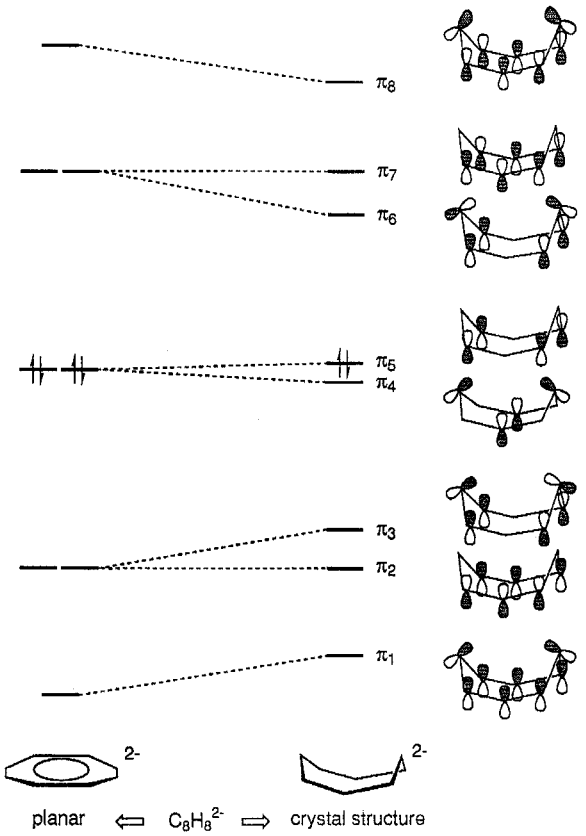

Figure 4. Orbital diagram showing the $C_8H_8^{2-}$ π orbitals' energy and their character upon undergoing a distortion from planarity to the tub shape ligand that is seen to straddle the W−W moiety in $W_2(COT)(NMe_2)_4$.

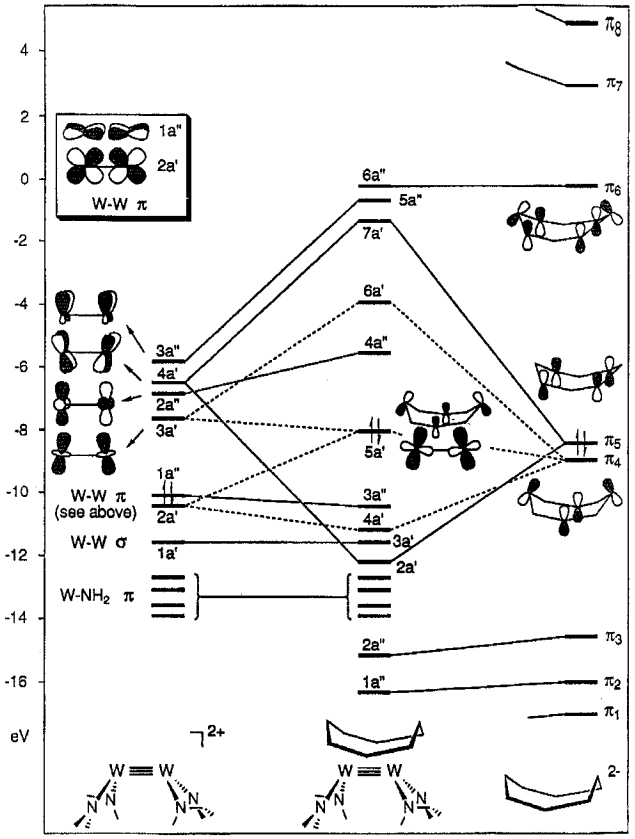

Figure 5. Orbital interaction diagram showing the key orbitals involved in forming $W_2(C_8H_8)(NH_2)_4$ from bent $C_8H_8^{2-}$ and $W_2(NH_2)_4^{2+}$ fragments.

Experimental Section

All manipulations were carried out under an atmosphere of dry nitrogen and solvents were thoroughly degassed and distilled from sodium benzophenone ketyl prior to use. 1,3,5,7-Cyclooctatetraene was purchased from Aldrich. $Li_2C_8H_8(THF)_x$[10] and $W_2Cl_2(NMe_2)_4$[11] were prepared according to published procedures.

NMR spectra were recorded on Bruker AM500 and Varian XL300 instruments. Variable-temperature spectra were calibrated by using MeOH. Infrared spectra were measured on a Perkin-Elmer 283 spectrophotometer.

Synthesis of $W_2(C_8H_8)(NMe_2)_4$. 1,2-$W_2Cl_2(NMe_2)_4$ (0.49 g, 0.79 mmol) was placed in a 100 mL Schlenk flask with a Teflon-coated magnetic stirring bar. Tetrahydrofuran (25 mL) was added and the solution cooled to 0 °C. $Li_2(C_8H_8)(THF)_x$ (0.29 g, 0.86 mmol) was added in small amounts from a solids addition tube (45 min). The reaction mixture was stirred for a further 1 $^1/_2$ h at 0 °C and for 3 h at room temperature. The solvent was removed *in vacuo*, and the residue was extracted with hexane and filtered through a bed of Celite on a medium-porosity frit. The hexane was removed *in vacuo*, and the residue was dissolved in toluene. Cooling of the toluene solution at −20 °C for 15 h afforded green crystals (yield 320 mg, 61.5% based on tungsten).

Anal. Calcd for $W_2C_{16}H_{32}N_4$ (648.2 g): C, 29.65; H, 4.98; N, 8.64. Found: C, 29.94; H, 5.10; N, 8.77.

IR data (Nujol mull between CsI plates) in cm^{-1}: 2854 (br, m), 2794 (m), 2752 (m), 1415 (m), 1406 (m), 1236 (m), 1226 (s), 1143 (ms), 1139 (sh, ms), 1130 (s), 1114 (sh, w), 1072 (w), 1047 (m), 1041 (m), 1033 (ms), 967 (vs), 952 (vs), 944 (vs), 932 (sh, s), 867 (m), 836 (vw), 827 (vw), 812 (s), 720 (vw), 681 (w), 554 (s), 462 (vw), 414 (vw), 371 (w), 325 (m), 309 (w), 296 (vw), 282 (vw), 271 (vw), 257 (vw).

^{1}H NMR data (toluene-d_8, 500 MHz, δ): 20 °C, 5.0 (very broad, $H_{(a)}-H_{(g)}$), 3.12 (br, only substantial resonance, NMe_2, $NMe_{2(a)}$, $NMe_{2(b)}$); 0 °C, 5.5 (very broad, 3H, $H_{(a)}-H_{(c)}$), 3.27 (s, 24H, NMe_2), 3.18 (br, 2H, $H_{(d)}$), 3.07 (s, 12H, $NMe_{2(b)}$), 3.01 (s, 12H, $NMe_{2(a)}$), 2.20 (br, 2H, $H_{(f)}$), 0.95 (br, 2H, $H_{(e)}$); −20 °C, 7.19 (m, 2H, $H_{(g)}$), 5.8 (br, 2H, $H_{(b)}$), 5.3 (br, 4H, $H_{(a)}$), 3.8 (br, 2H, $H_{(c)}$), 3.31 (s, 24H, NMe_2), (3.20 (dd, 2H, $H_{(d)}$), 3.08 (s, 12H, $NMe_{2(b)}$), 3.02 (s, 12H, $NMe_{2(a)}$), 2.23 (d, 2H, $H_{(f)}$), 0.98 (d, 2H, $H_{(e)}$); −40 °C, 7.25 (m, 2H, $^3J_{H_{(g)}-H_{(f)}} < 2$ Hz, $^4J_{H_{(g)}-H_{(f)}} < 2$ Hz, $H_{(g)}$, 5.80 (t, 2H, $^3J_{H_{(b)}-H_{(a)}} = 8$ Hz, $H_{(b)}$), 5.29 (dd, 4H, $^3J_{H_{(a)}-H_{(c)}} = 10$ Hz, $H_{(a)}$), 3.77 (t, 2H, $H_{(c)}$), 3.34 (s, 24H, NMe_2), 3.22 (dd, 2H, $^3J_{H_{(d)}-H_{(e)}} = 3$ Hz, $^4J_{H_{(d)}-H_{(e)}} = 2$ Hz, $H_{(d)}$), 3.10 (br s, 12H, $NMe_{2(b)}$), 3.02 (s, 12H, $NMe_{2(a)}$), 2.26 (ddd, 2H, $^3J_{H_{(f)}-H_{(e)}} = 12$ Hz, $H_{(f)}$), 1.00 (ddd, 2H, $H_{(e)}$).

^{13}C NMR (126 MHz, toluene-d_8, −40 °C, δ): 138.9 (d, $^1J_{C-H} = 156$ Hz, COT), 97.5 (d, $^1J_{C-H} = 173$ Hz, COT), 96.4 (dt, $^1J_{C-H} = 161$ Hz, $^3J_{C-H} = 9$ Hz, COT), 75.0 (dt, $^1J_{C-H} = 148$ Hz, $^3J_{C-H} = 10$ Hz, $J_{W-C} = 20$ Hz, 20%, COT), 66.5 (dt, $^1J_{C-H} = 150$ Hz, $^3J_{C-H} = 8$ Hz, COT), 65.2 (d, $^1J_{C-H} = 172$ Hz, COT), 52.4 (qq, $^1J_{C-H} = 132$ Hz, $^4J_{C-H} = 6$ Hz, NMe_2), 49.4 (d, $^1J_{C-H} = 155$ Hz, COT), 48.0 (q, $^1J_{C-H} = 133$ Hz, NMe_2), 47.0 (qq, $^1J_{C-H} = 133$ Hz, $^4J_{C-H} = 6$ Hz, NMe_2).

X-ray Crystallographic Studies. General operating procedures and listings of programs have been given.[12] A summary of crystal data is presented in Table 4.

A suitable small crystal (approximately 0.24 × 0.26 × 0.20 mm in size) was cleaved from a larger cluster of crystals. The crystal was transferred to the goniostat where it was cooled to −143 °C for characterization and data collection. A sys-

(10) Spencer, J. L. *Inorg. Synth.* **1979**, *19*, 214. The molarity of $Li_2C_8H_8(THF)_x$ was determined by treating a known mass of the sample with H_2O and titrating the LiOH against a standardized solution of HCl.

(11) Akiyama, M.; Chisholm, M. H.; Cotton, F. A.; Extine, M. W.; Murillo, C. A. *Inorg. Chem.* **1977**, *16*, 2407.

(12) Chisholm, M. H.; Folting, K.; Huffman, J. C.; Kirkpatrick, C. C. *Inorg. Chem.* **1984**, *23*, 1021.

Table 4. Summary of Crystal Data

empirical formula	$C_{16}H_{32}N_4W_2$
color of cryst	green
cryst dimens (mm)	0.24 × 0.26 × 0.20
space group	$P2_1/a$
temp (°C)	−143
cell dimens	
a (Å)	8.028(1)
b (Å)	30.784(3)
c (Å)	8.538(1)
β (deg)	116.55(1)
Z (molecules/cell)	4
V (Å)	1887.33
calcd density	2.281
wavelength (Å)	0.710 69
M_r	648.16
linear abs coeff	124.481
detector to sample dist (cm)	22.5
sample to source dist (cm)	23.5
av ω scan width at half-height	0.25
scan speed (deg/min)	6.0
scan width (deg + dispersion)	1.4
individual bckgd (s)	7
aperture size (mm)	3.0 × 4.0
2θ range (deg)	6−55
tot. no. of reflcns collcd	5640
no. of unique intensities	4277
no. with $F > 0.0$	4140
no. with $F > 3\sigma(F)$	4056
$R(F)$	0.0443
$R_w(F)$	0.0451
goodness of fit for the last cycle	2.470
max δ/σ for the last cycle	0.05

tematic search of a limited hemisphere of reciprocal space carried out by using a newly installed computer−controlled search procedure yielded a set of reflections which exhibited monoclinic diffraction symmetry (2/*m*). The systematic extinctions of 0*k*0 for $k = 2n + 1$ and of *h*0*l* for $h = 2n + 1$ uniquely determined the space group as $P2_1/a$ (an alternate setting of space group No. 14). Data collection were undertaken as detailed in Table 4. Due to the long *b*-axis a scan width of 1.4° plus dispersion was used. The crystal diffracted very strongly, and the upper limit for the data collection was extended to 55°. A total of 5640 reflections were collected. Four standard reflections monitored periodically during the data collection showed no systematic trends. During the data processing it was noted that a few of the reflections had abnormally high background counts, most likely due to the presence of a crystal fragment. The raw data were scanned carefully, and most of the reflections suffering from the bad background counts were removed. In most cases the reflections were observed twice and the redundant reflection did not have abnormal background counts. After averaging the redundant data a unique set of 4277 reflections remained. Of these 4056 were considered observed by the criterion $F > 3.0\sigma(F)$. The *R* for the averaging was 0.03 for 1175 redundant data.

The data were corrected for absorption as detailed in Table 4. The absorption correction did not improve the final difference map as much as had been expected, most likely due to the presence of the fragment.

The structure was solved in the usual manner using a combination of direct methods and Fourier techniques. The two tungsten atoms were located in the best *E*-map following MULTAN, and the remaining non-hydrogen atoms were located in a difference Fourier phased with the W atoms. All of the hydrogen atoms on the cyclooctatetraene were located in a subsequent difference map as were almost all of the hydrogens on the methyl groups. The hydrogen atoms on the methyl groups were introduced in idealized positions, and the full-matrix least-squares refinement was completed using anisotropic thermal parameters on the non-hydrogen atoms and isotropic thermal parameters on the hydrogen atoms. The final *R* was 0.043.

The final difference map contained a few peaks of approximately 3.0 e/Å^3 in the vicinity of the W atoms. Otherwise the map was essentially featureless.

Computational Procedures. Molecular orbital calculations were performed on a VAX computer system with the Fenske−Hall approximate MO method.[13] All atomic wave functions used were generated by the method of Bursten, Jensen, and Fenske.[14] Contracted double-ζ representations were used for the W 5d, N 2p, and C 2p AOs. The W 6s and 6p exponents were fixed at 2.40. All calculations were converged with a self-consistent-field interactive technique by using a convergence criteria of 0.0010 as the largest deviation between atomic orbital populations for successive cycles.

The model compound, $W_2(COT)(NH_2)_4$, was constructed from interactomic distances and angles taken from the crystal structure of $W_2(COT)(NMe_2)_4$ and idealized to C_2 symmetry. The N−H bond lengths were set at 1.02 Å.

Acknowledgment. We thank the National Science Foundation for support. R.H.C. was the recipient of an NSF postdoctoral fellowship, 1989−1992. K.G.M. thanks the University of Durban-Westville for a leave of absence. We thank Dr. Theodore Budzichowski for helpful discussions and for pointing out that structure **IIb** also accounts for the observed NMR spectrum of the minor isomer.

Supporting Information Available: Listings of anisotropic thermal parameters and complete bond distances and bond angles (4 pages). Ordering information is given on any current masthead page.

OM9508748

(13) Hall, M. B.; Fenske, R. F. *Inorg. Chem.* **1972**, *11*, 768.
(14) Bursten, B. E.; Jensen, J. R.; Fenske, R. F. *J. Chem. Phys.* **1978**, *68*, 3320.